Supporting Information

Oxytocin-monolayer based impedimetric biosensor for zinc and copper ions

Kiran Kumar Tadi,[a,b] Israel Alshanski,[a,b] Evgeniy Mervinetskiy,[a,b] Gerard Marx,[c] Panayiota Petrou,[d] Karussis M. Dimitrios,[d] Chaim Gilon,[a] Mattan Hurevich,[*a] and Shlomo Yitzchaik[*a,b]

[*a]Institute of Chemistry and the [b]Center for Nanoscience and Nanotechnology, the Hebrew University of Jerusalem, Jerusalem-9190401 Israel

[c]MX Biotech Ltd., Jerusalem 95744, Israel

[d]Department of Neurology, Hadassah-Hebrew University Hospital, Ein Kerem, Jerusalem 91120, Israel.

[*]*Correspondence E-mail:* shlomo.yitzchaik@mail.huji.ac.il
mattan.hurevich@mail.huji.ac.il

TABLE OF CONTENTS

Contents

EXPERIMENTAL SECTION S3
S1. Synthesis of N(2-azidoacetyl)-oxytocin (OT-AZ) S3
S1.1 Solid phase synthesis of the protected linear peptide S3
2-azidoacetyl-Cys(Trt)-Tyr(t-Bu)- S3
S1.2 Coupling S3
S1.3 Fmoc deprotection S3
S1.4 Peptide Cyclization S3
S1.5 Peptide cleavage S4
S1.6 Purification of OT azide S4
S1.7 Mass Spectrometry analysis of OT azide S4
S2. Characterization of the OT-Wafer S4
S3. Electrochemical measurements S5
RESULTS AND DISCUSSION S6
S4.1 IR Spectroscopy S6
S4.2 Chronocouloumetry ..... S**Error! Bookmark not defined.**
Tables S7
Figures S8
REFERENCES S11
6

EXPERIMENTAL SECTION

S1. Synthesis of N(2-azidoacetyl)-oxytocin (OT-AZ)

S1.1 Solid phase synthesis of the protected linear peptide

2-azidoacetyl-Cys(Trt)-Tyr(t-Bu)-**Ile-Gln(Trt)-Asn(Trt)-Cys(Trt)-Pro-Leu-Gly-Rink Amide MBHA Resin.** Syntheses was performed in a reaction vessel equipped with a sintered glass bottom applying general Fmoc chemistry protocols for SPPS in a microwave reactor: Fmoc rink amide methylbenzhydrilamine (Fmoc-MBHA) resin (0.25g, 0.71 mmol/g was treated with 20% piperidine in NMP solution for 1 h and followed by washing with NMP (3 × 2 min.)

S1.2 Coupling

Coupling to the N-terminus of the growing peptide was performed using the following method: Fmoc-[Amino Acid]-OH (3 equiv.) was dissolved in N-methyl-2-pyrrolidone (NMP), HATU (3 equiv.) and *N,N*-Diisopropylethylamine (8 equiv.) were added to the solution for pre-activation and shaken for 3 min. The pre-activated solution was poured onto the resin and micro waved (5 min, 85°C) followed by washing with NMP (3 × 2 min). After the removal of the Fmoc group from the terminal Lys, 2-azido acetic acid was coupled to the free amine using HATU as coupling agent.

S1.3 Fmoc deprotection

Fmoc deprotection was performed by mixing` the resin with 20% piperidine in NMP solution (micro wave, 5 min, 85°C). After washing with NMP (3 × 2 min.) the following Fmoc amino acid in the sequence was coupled as described in section a. above. The equivalents of all reagents were in respect to the resin weight and loading capacity, and the volume of the SPPS solvents used in most of the reactions was between 7-10 mL.

S1.4 Peptide Cyclization

10 mL of 10 equivalents of Iodine in 2% v/v anisole/NMP solution was added to the peptidyl-resin and micro-waved for 5 minutes and washed with NMP (3×2 min).

S1.5 Peptide cleavage

The resin was washed with NMP (3×2 min), isopropanol (3×2 min) and ether (3×2 min). The resin was dried in vacuum. Cleavage from the resin and simultaneous removal of side chain protecting groups was carried out using a standard 10 ml cocktail composed of 95% trifluoroacetic acid (TFA), 2% triply distilled water (TDW), 1% triisopropylsilane (TIS) 2% TDW, 1% TIS and 2% and 1,2 ethanedithiol. The cocktail was added to about 0.7 g the dry peptidyl-resin. The mixture was mixed for 4 hours at room temperature. The resin was removed by filtration and was washed with 3 ml TFA 3 times. The combined TFA filtrate (with the peptide dissolved in it) was partially evaporated by a stream of nitrogen to a small volume (~5mL). Cold diethyl ether (30 mL) was added to remove scavengers and other hydrophobic side products, and the peptide was precipitated by centrifugation. Diethyl ether was then removed by decantation. The solid peptide was vortexed with cold diethyl ether (30 mL) and centrifugation and decantation. The process was repeated three times. The crude peptide was dried in vacuum, dissolved in acetonitrile (ACN/TDW 1:1 v/v) and lyophilized overnight.

S1.6 Purification of OT azide

The peptide was purified by gradient RP-HPLC, going from 5% ACN in TDW to 90% ACN in TDW within 40 minutes. The peak with the product collected manually. Analytical HPLC analysis shows pure OT azide after purification at gradient of 5% ACN to 70% CAN in TDW and the corresponding high resolution mass spectrum of OT azide is shown in Figure S1.

S1.7 Mass Spectrometry analysis of OT azide

High resolution mass spectrometry performed on Agilent 6550 iFunnel Q-TOF LC/MS system and is shown in Figure S1.

S2. Characterization of the OT-Wafer

Spectroscopic ellipsometry is a convenient and accurate technique for the measurement of thickness and optical constants based on the changes in the state of polarization light upon reflection of light from a surface.[2] The thicknesses of the modified silicon wafer were determined using a J.A. Woollam Company VASE® variable angle spectroscopic ellipsometer. Optical

modelling and data analysis were done using the Woollam Company WVASE32™ software package.[3] Ellipsometric Ψ and Δ data were acquired on silicon substrate at three angles of incidence 75° over the spectral range 300–900 nm (0.73–4.13 eV) in steps of 10 nm**.** Cauchy model was considered to fit the ellipsometric plot obtained after modification of Si/SiO_2. Surface topography of modified silicon wafer was measured (1 μm × 1 μm) with an atomic force microscope (Innova, Bruker) in tapping mode using FESPA-V2 probes having tip radius of 12 nm. Several macroscopically distant locations on each sample were scanned to eliminate "local effects". The adsorption of Zn^{2+} and Cu^{2+} ions to the OT-Wafer was confirmed using Axis Ultra X-ray photoelectron spectrometer. Fourier transform infrared (FT-IR) spectra were recorded with a Bruker Vertex 70v spectrometer in a reflection mode (80˚) using a liquid-nitrogen-cooled mercury cadmium telluride (MCT) detector. The samples were scanned 1023 times with 4 cm^{-1} resolution.

S3. Electrochemical measurements

Electrochemical impedance studies (EIS) were conducted using a Biologic potentiostat, model SP-300. The EIS measurements were conducted in the 3-electrode system consists of glassy carbon electrode (GCE) as working electrode and Ag/AgCl (Sat. KCl) as reference electrode and spiral platinum wire as counter electrode. All EIS measurements were carried out in room temperature at half-wave peak potential (0.210 V) of the redox mixture in phosphate buffer solution (100 mM, pH 7.0) containing a mixture of 5 mM $[Fe(CN)_6]^{4-}$ and 5 mM $[Fe(CN)_6]^{3-}$. The AC frequency was scanned ranging from 100 kHz to 0.01 Hz with excitation amplitude of 10 mV. Using the redox probe (5 mM $[Fe(CN)_6]^{3-/4}$), the change in charge transfer resistance (R_{CT}) at electrode/electrolyte interface has been investigated by EIS. Generally, EIS spectra of self-assembled monolayers (SAM) on electrodes are analyzed by fitting the plots with Randles equivalent circuit in which capacitance (C_{dl}) is replaced by constant phase element (CPE). The position of the reference electrode and the OT-Sensor was kept the same to minimize the variation in solution resistance (R_s). The OT-Sensor was immersed into the desired concentration of Zn^{2+}/Cu^{2+} ion solution for 5 minutes. Subsequently the electrode was washed twice with working buffer to remove non-specific bound ions.

The parallel detection of Zn^{2+} and Cu^{2+} coexisting in a sample was achieved by using 10 μM thiourea and 10 μM pyrophosphate for masking Cu^{2+} and Zn^{2+} respectively.[4,5]

RESULTS AND DISCUSSION

S4.1 IR Spectroscopy

Figure S5 presents the reflectance absorbance IR spectra of Si-wafer modified at various modifications. As is observed from the spectra, APTES modified Si-wafer doesn't show any major peaks due to low dense layer of APTES. However after coupling of DBCO through amide linking, a significant peak in 2118 cm^{-1} (red colored) contributed to alkyne (C≡C) bond stretching.[6] The alkyne peak disappears after OT incubation (blue colored) as alkyne presented in DBCO is coupled with azide functionality of OT to form triazole ring (click chemistry). The click reaction is further evident from the peak at 3140 cm^{-1} associated to the stretching of the C=C bonds in the triazole.[7] Additional peaks in the range of 1400-1800 cm^{-1} corresponding to changes in C=O and C=C aromatic stretches[8] results in OT coupling. Broad peaks in the range of 2818 cm^{-1} to 3020 cm^{-1} are related to differences in C-H stretching[9,10] of DBCO and OT surface modification step. In this way, the FTIR spectra support the applied surface modification steps for anchoring OT onto the surface.

Tables

Table S1. Ellipsometric thickness of the various layers assembly steps of OT-wafer.

Layer (step #)[a]	Thickness (Å)[b]
Wafer (Si/SiO_2)	25.05 (±0.83)
Wafer-$PrNH_2$ (step 1)	7.80 (± 0.34)
Wafer-DBCO (step 2)	6.50 (± 0.62)
OT-Wafer (step 3)	33.40 (± 0.55)

[a]The step # are the same steps shown in Figure S2 applied to silicon wafer.

[b]The values in the parentheses indicate the RSD values based on three replicate measurements.

Table S2. Reproducibility and precision of the OT-Sensor

Electrode No.	Zn^{2+}			Cu^{2+}		
	Conc. found (M)	Standard deviation (%)	Coefficient of variation (%)	Conc. found (M)	Standard deviation (%)	Coefficient of variation (%)
1	2.82×10^{-09}	2.75	1.80	2.20×10^{-09}	3.23	1.93
2	2.54×10^{-09}			2.10×10^{-09}		
3	5.83×10^{-09}			8.79×10^{-10}		
4	1.02×10^{-08}			1.72×10^{-09}		
5	3.85×10^{-09}			3.05×10^{-09}		

Figures

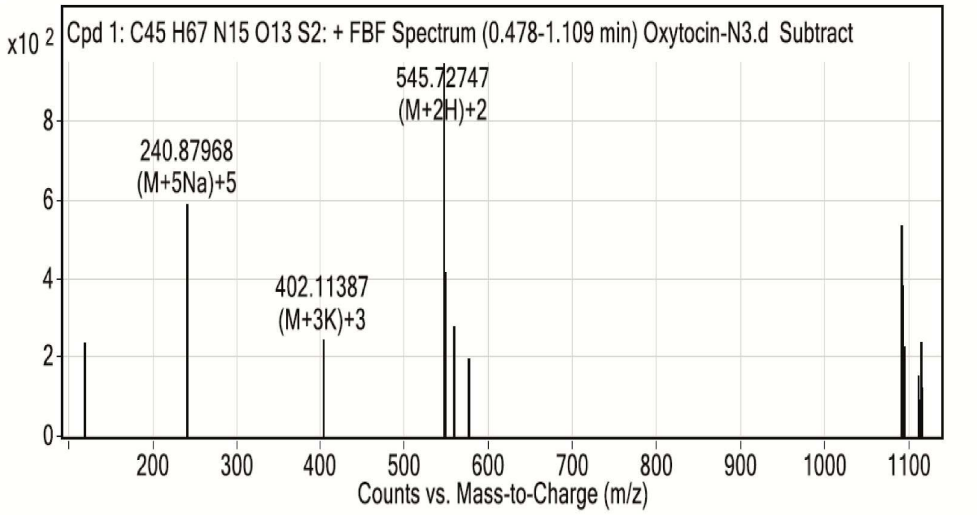

Figure S1. Mass spectra of azidoacetamide-oxytocin (OT-AZ).

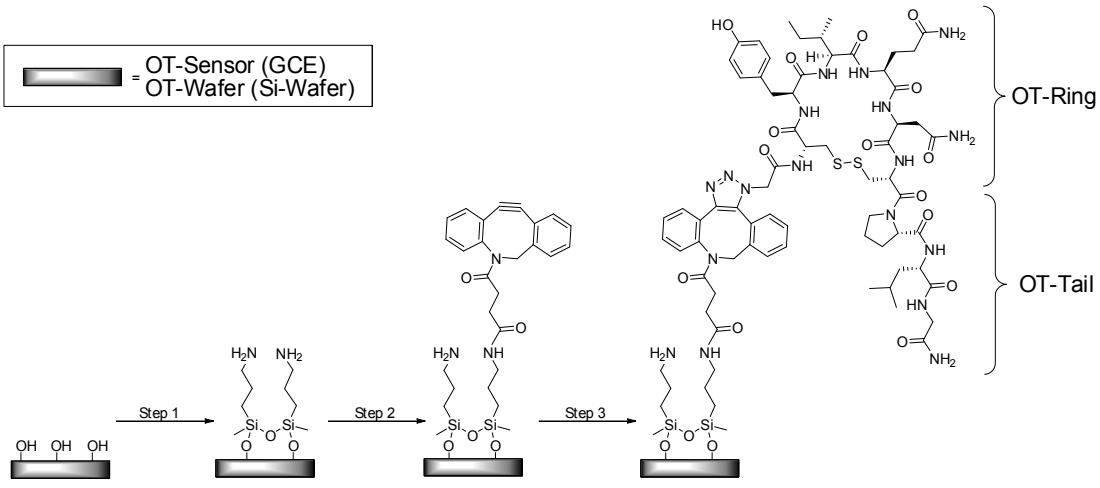

Figure S2. General scheme of OT-Sensor/OT-Wafer step wise preparation; step 1) APTES modification on GCE/Si-Wafer active hydroxyl, step 2) DBCO-NHS coupling to the amine on the interface, step 3) Azido-OT coupling to DBCO by click chemistry.

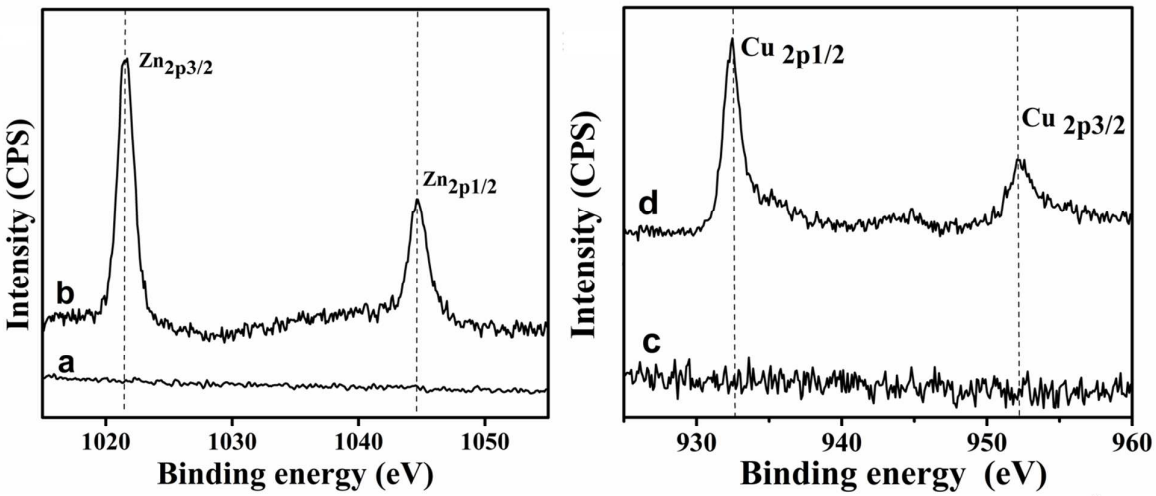

Figure S3. XPS spectra of OT-Wafer before (a and c) and after incubation in (b) 1 μM Zn^{2+} and (d) 1 μM Cu^{2+} solution.

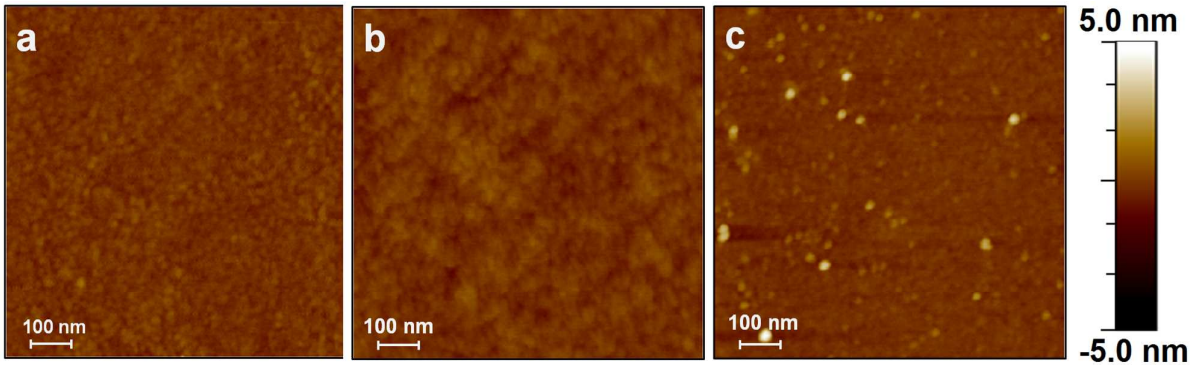

Figure S4. Atomic force microscopic images (area: 1.0 μm × 1.0 μm) recorded for OT immobilized Si/SiO_2 (OT-Wafer): (a) hydroxylated silicon wafer (ρ=2.0 Å), (b) APTES modified silicon wafer (ρ=2.2 Å), (c) DBCO modified silicon wafer (ρ=2.5 Å).

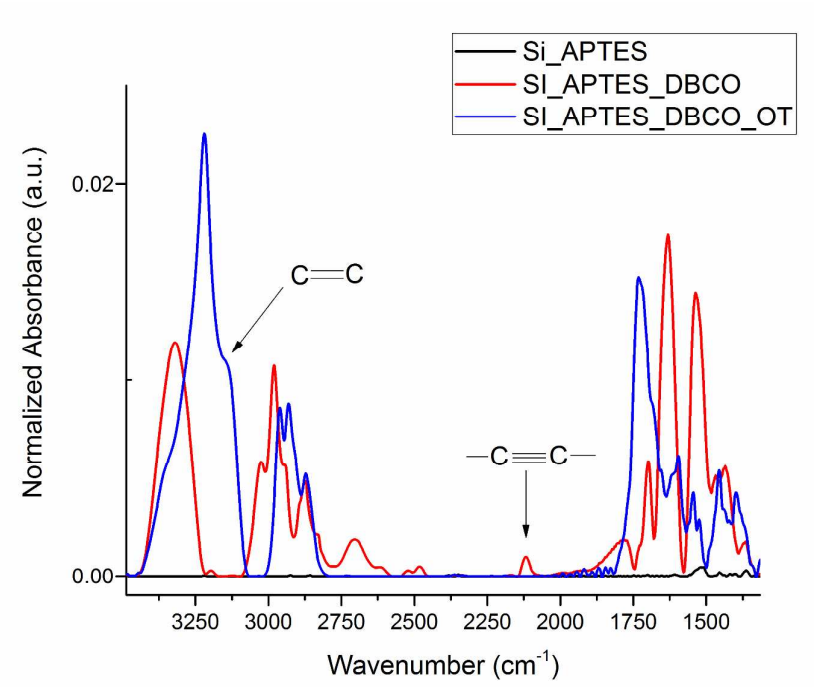

Figure S5. FT-IR spectra of Si-APTES surface (black), Si-APTES after DBCO coupling (red) and Si-APTES-DBCO after OT incubation (blue)**.**

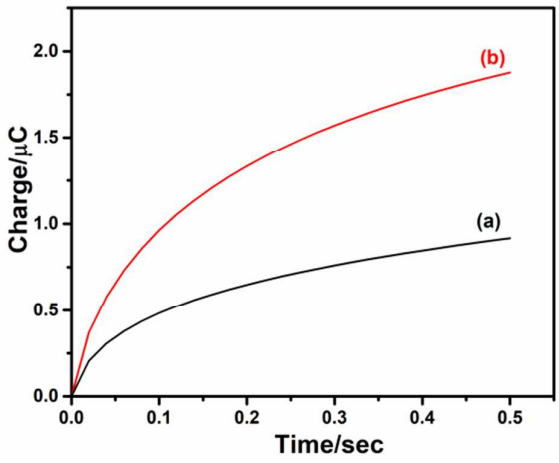

Figure S6. Chronocoulometric responses of OT-GCE performed in the absence (a) and presence (b) of 50 μM Fe^{2+}/Fe^{3+} redox probe

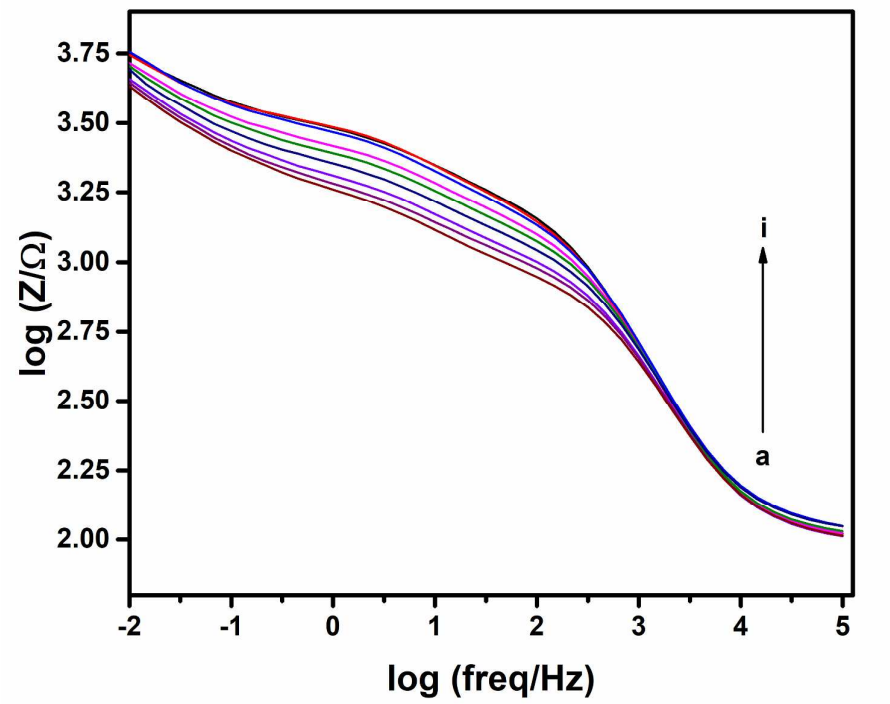

Figure S7. Bode plots of impedance spectroscopy for the OT-Sensor after incubation in various Zn^{2+} concentrations; (a) blank solution (b) 2.5×10^{-12} M Zn^{2+} (c) 7.5×10^{-11} M Zn^{2+} (d) 1.0×10^{-12} M Zn^{2+} (e) 1.0×10^{-11} M Zn^{2+} (f) 1.0×10^{-10} M Zn^{2+} and (g) 1.0×10^{-9} M Zn^{2+} (h) 1.0×10^{-8} M Zn^{2+} and (i) 1.0×10^{-7} M Zn^{2+} (Supporting electrolyte: 5 mM $[Fe(CN)_6]^{3-/4-}$ consists of 0.1 M PBS at pH 7.0)

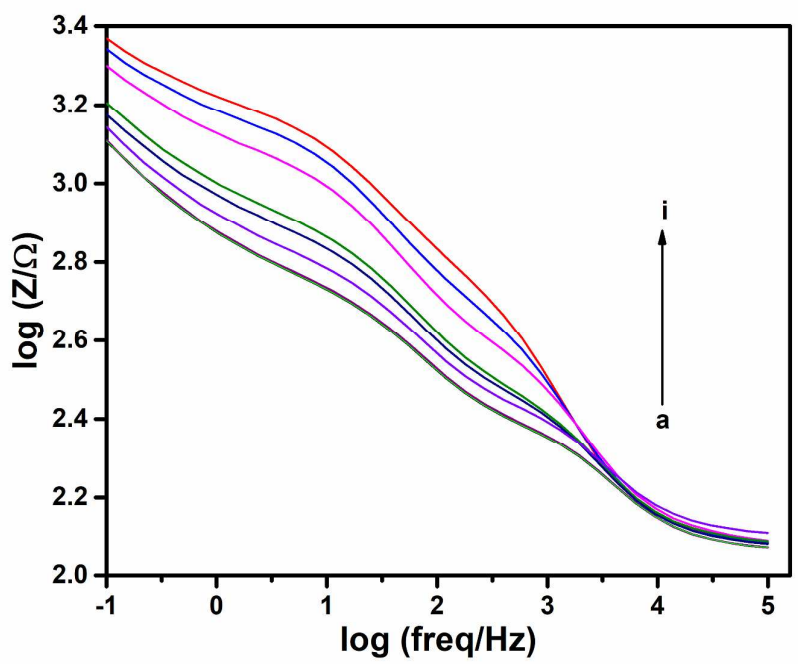

Figure S8. Bode plots of impedance spectroscopy for the OT-Sensor after incubation in various Cu^{2+} concentrations; (a) blank solution (b) 1.0×10^{-12} M Cu^{2+} (c) 1.0×10^{-11} M Cu^{2+} (d) 1.0×10^{-10} M Cu^{2+} (e) 1.0×10^{-9} M Cu^{2+} (f) 1.0×10^{-8} M Cu^{2+} (g) 1.0×10^{-7} M Cu^{2+} and (i) 1.0×10^{-7} M Cu^{2+} (Supporting electrolyte: 5 mM $[Fe(CN)_6]^{3-/4-}$ consists of 0.1 M PBS at pH 7.0)

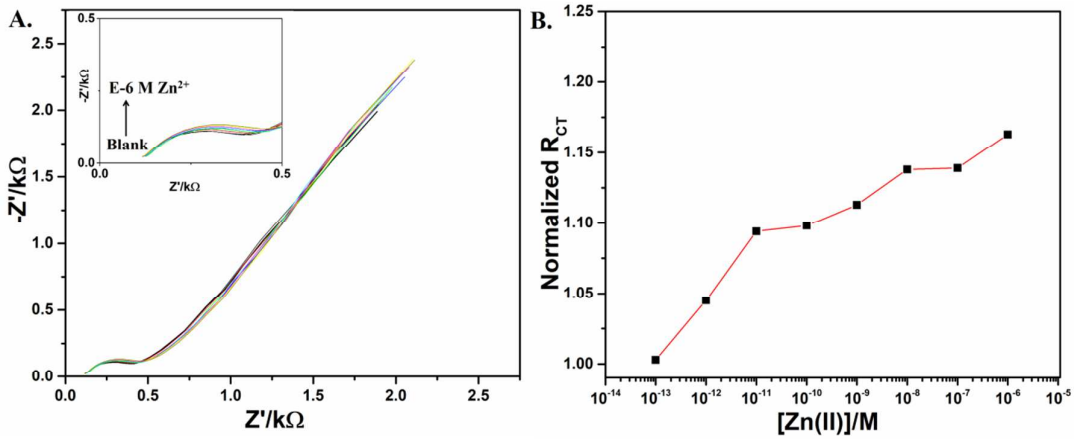

Figure S9. (A) Nyquist plots obtained for GCE-DBCO in 5 mM $[Fe(CN)_6]^{3-/4-}$ consists of 0.1 M PBS at pH 7.0 after incubation in various Zn^{2+} concentrations; blank solution, 1.0×10^{-13} M Zn^{2+}, 1.0×10^{-12} M Zn^{2+}, 1.0×10^{-11} M Zn^{2+}, 1.0×10^{-10} M Zn^{2+}, 1.0×10^{-9} M Zn^{2+}, 1.0×10^{-8} M Zn^{2+}, 1.0×10^{-7} M Zn^{2+}, 1.0×10^{-6} M Zn^{2+} (inset: enlarged Nyquist plots) (B) logarithmic concentration of Zn^{2+} vs. normalized charge transfer resistance (R_{CT}).

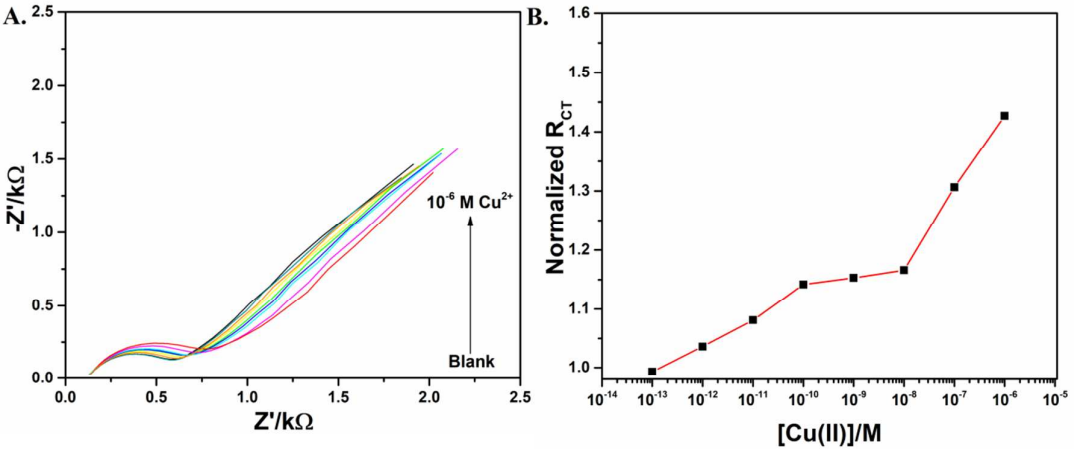

Figure S10. (A) Nyquist plots obtained for GCE-DBCO in 5 mM $[Fe(CN)_6]^{3-/4-}$ consists of 0.1 M PBS at pH 7.0 after incubation in various Cu^{2+} concentrations; blank solution, 1.0×10^{-13} M Cu^{2+}, 1.0×10^{-12} M Cu^{2+}, 1.0×10^{-11} M Cu^{2+}, 1.0×10^{-10} M Cu^{2+}, 1.0×10^{-9} M Cu^{2+}, 1.0×10^{-8} M Cu^{2+}, 1.0×10^{-7} M Cu^{2+}, 1.0×10^{-6} M Cu^{2+} (inset: enlarged Nyquist plots) (B) logarithmic concentration of Zn^{2+} vs. normalized charge transfer resistance (R_{CT})

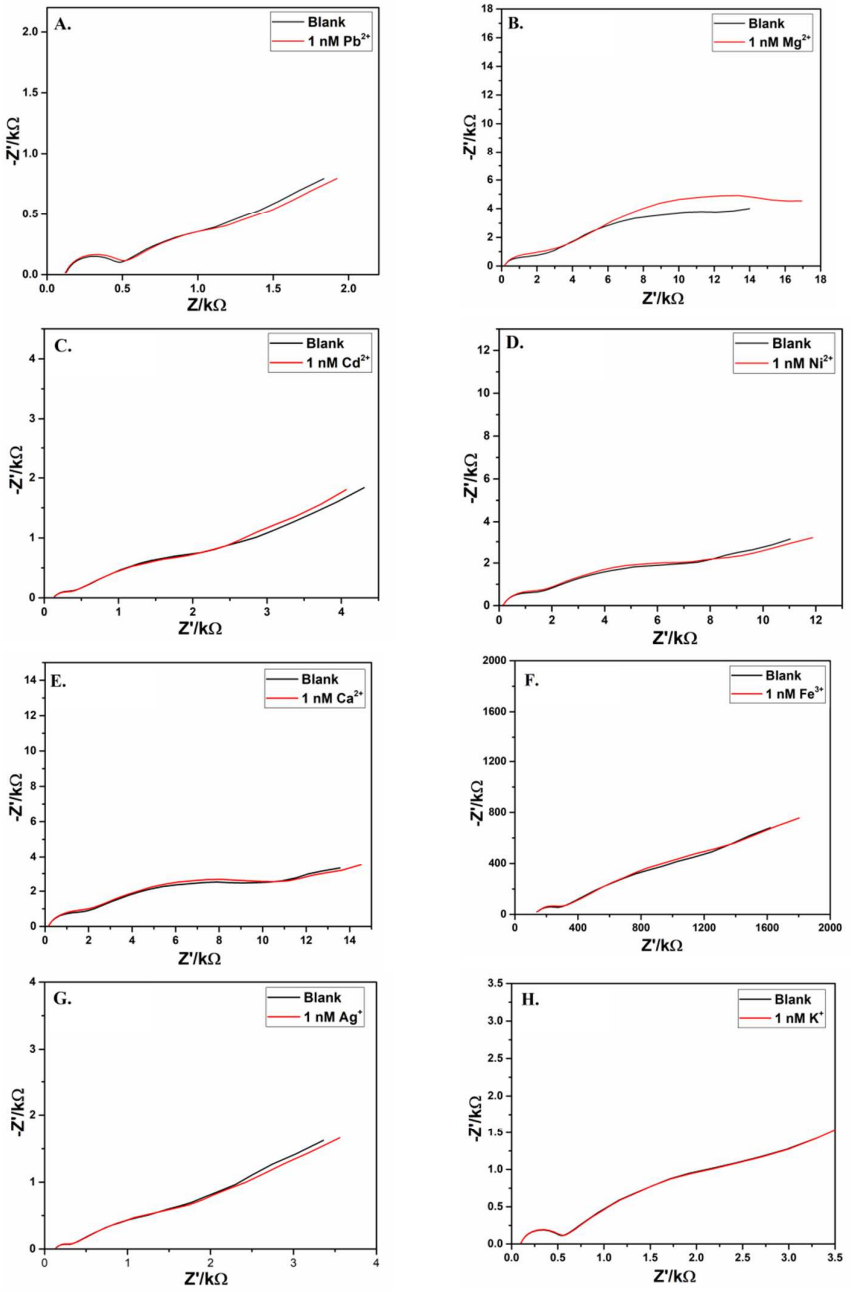

Figure S11. Nyquist plots obtained OT-GCE sensor in the absence and presence of 1 nM metal ions (A) Pb^{2+} (B) Mg^{2+} (C) Cd^{2+} (D) Ni^{2+} (E) Ca^{2+} (F) Fe^{3+} (G) Ag^{+} and (H) K^{+}

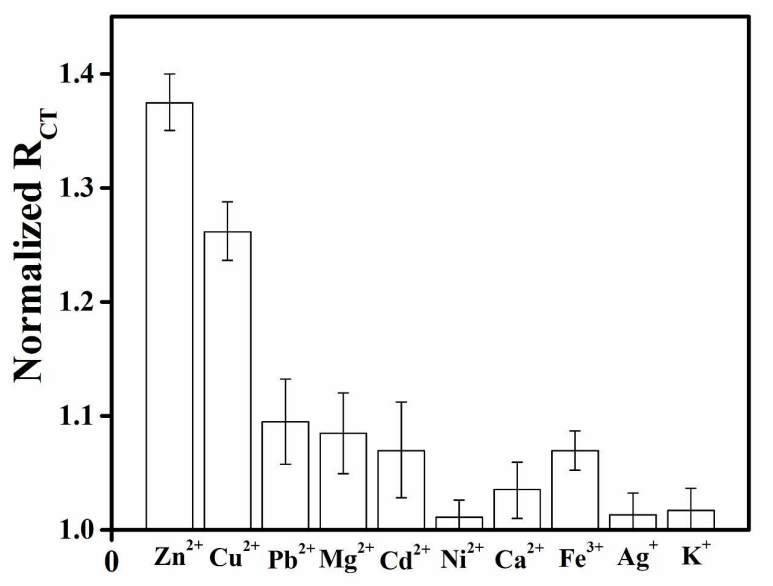

Figure S12. Response of the OT-Sensor towards various metal ions in 1nM concentration

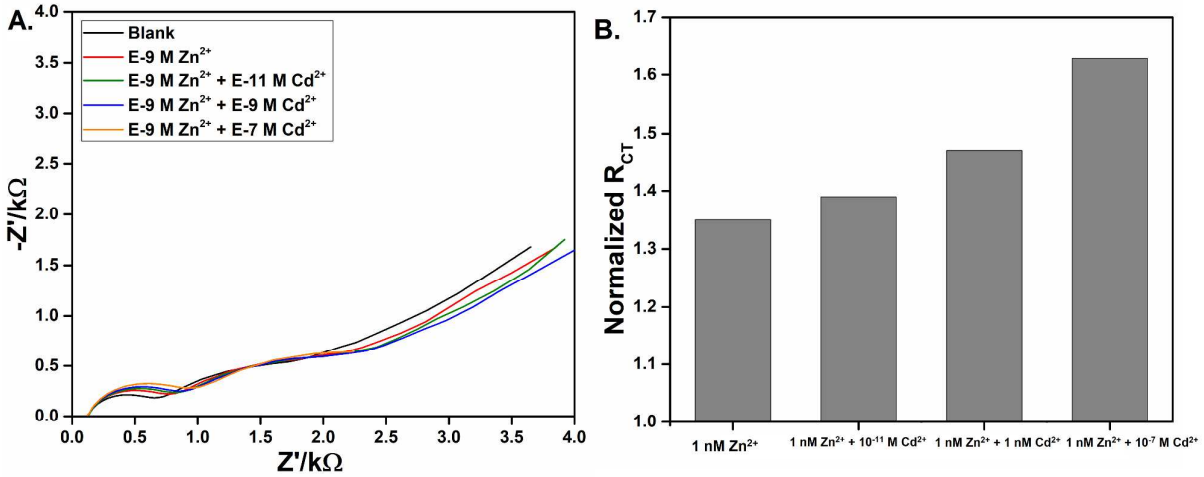

Figure S13. (A) Nyquist plots obtained for 1 nM Zn^{2+} in presence of various concentrations of Cd^{2+} and (B) the corresponding histogram showing normalized R_{CT} vs. various concentration of Cd^{2+} in presence of 1 nM Zn^{2+}

REFERENCES

1. W. Kern, and J. E. Soc, *J. Electrochem. Soc.* 1990, **137,** 1887–1892.

2. H. Fujiwara, *Spectroscopic Ellipsometry: Principles and Applications*, John Wiley & Sons, Ltd, 2007.

3. J. A. Woollam Co. *WVASE Manual* 2012.

4. C. G Halliday, and M. A. Leonard. *Analyst* 1987, **112,** 329–332.

5. P. Das, N. B. Chandar, S. Chourey, H. Agarwalla, B. Ganguly, and A. Das, *Inorg. Chem.* 2013**, 52** (19), 11034–11041.

6. Sun, D.; Miao, X.; Zhang, K.; Kim, H.; Yuan, Y. Triazole-Forming Waterborne Polyurethane Composites Fabricated with Silane Coupling Agent Functionalized Nano-Silica. *J. Colloid Interface Sci.* **2011**, *361*, 483–490.

7. Wu, Y.-C.; Kuo, S.-W. Synthesis and Characterization of Polyhedral Oligomeric Silsesquioxane (POSS) with Multifunctional Benzoxazine Groups through Click Chemistry. *Polymer (Guildf).* **2010**, *51*, 3948–3955.

8. Wang, Y.; Chen, J.; Xiang, J.; Li, H.; Shen, Y.; Gao, X.; Liang, Y. Synthesis and Characterization of End-Functional Polymers on Silica Nanoparticles via a Combination of Atom Transfer Radical Polymerization and Click Chemistry. *React. Funct. Polym.* **2009**, *69*, 393–399.

9. Wang, H.; Jiang, P.; Zhang, M.; Dong, X. Synthesis of a Novel Restricted Access Chiral Stationary Phase Based on Atom Transfer Radical Polymerization and Click Chemistry for the Analysis of Chiral Drugs in Biological Matrices. *J. Chromatogr. A* **2011**, *1218*, 1310–1313.

10. Quémener, D.; Hellaye, M. Le; Bissett, C.; Davis, T. P.; Barner-Kowollik, C.; Stenzel, M. H. Graft Block Copolymers of Propargyl Methacrylate and Vinyl Acetate via a Combination of

RAFT/MADIX and Click Chemistry: Reaction Analysis. *J. Polym. Sci. Part A Polym. Chem.* **2008**, *46*, 155–173.

11. Adam B. Steel; Tonya M. Herne; Michael J. Tarlov, Electrochemical Quantitation of DNA Immobilized on Gold. *Analytical Chemistry,* **2008,** *70,* 4670-4677.
12. Tadi K. K.; Motghare R. V. Voltammetric Determination of Pindolol in Biological Fluids Using Molecularly Imprinted Polymer Based Biomimetic Sensor *Journal of The Electrochemical Society*, **2016**, *163*, B286-B292.
13. A. J. Bard and L. R. Faulkner, *Electrochemical Methods: Fundamentals and Applications*, **20104,** p. 104, John Wiley& Sons, New York.